Open access • Journal Article • DOI:10.1016/J.COLSURFA.2017.12.043

Magnetic metal organic frameworks (MOFs) composite for removal of lead and malachite green in wastewater — Source link

Zhennan Shi, Chen Xu, Han Guan, Ling Li ...+6 more authors

Institutions: Hubei University, University of Science and Technology, Liaoning, University of Queensland

Published on: 20 Feb 2018 - Colloids and Surfaces A: Physicochemical and Engineering Aspects (Elsevier)

Topics: Freundlich equation and Adsorption

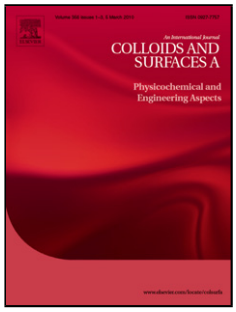

Title: Magnetic Metal Organic Frameworks (MOFs) Composite for Removal of Lead and Malachite Green in Wastewater

Authors: Zhennan Shi, Chen Xu, Han Guan, Ling Li, Lu Fan, Yingxi Wang, Li Liu, Qingtao Meng, Run Zhang

PII: S0927-7757(17)31140-8
DOI: https://doi.org/10.1016/j.colsurfa.2017.12.043
Reference: COLSUA 22167

To appear in: *Colloids and Surfaces A: Physicochem. Eng. Aspects*

Received date: 28-9-2017
Revised date: 17-12-2017
Accepted date: 18-12-2017

Please cite this article as: Shi Z, Xu C, Guan H, Li L, Fan L, Wang Y, Liu L, Meng Q, Zhang R, Magnetic Metal Organic Frameworks (MOFs) Composite for Removal of Lead and Malachite Green in Wastewater, *Colloids and Surfaces A: Physicochemical and Engineering Aspects* (2010), https://doi.org/10.1016/j.colsurfa.2017.12.043

Magnetic Metal Organic Frameworks (MOFs) Composite for Removal of Lead and Malachite Green in Wastewater

Zhennan Shi[a,b‡], *Chen Xu*[a,b‡], *Han Guan*[a,b], *Ling Li*[a,b*], *Lu Fan*[a,b], *Yingxi Wang*[a,b], *Li Liu*[a,b], *Qingtao Meng*[c], *Run Zhang*[c,d*]

[a] Hubei Collaborative Innovation Center for Advanced Organic Chemical Materials, Hubei University, Wuhan 430062, People's Republic of China

[b] Ministry-of-Education Key Laboratory for the Synthesis and Application of Organic Function Molecules, Hubei University, Wuhan City, Hubei Province 430062, People's Republic of China

[c] School of Chemical Engineering, University of Science and Technology Liaoning, Anshan, 114044, China

[d] Australian Institute for Bioengineering and Nanotechnology, The University of Queensland, Brisbane, 4072, Australia

[‡] These authors contributed equally to this work

* Corresponding authors

Dr. Ling Li, Email: waitingll@yahoo.com Phone: +86-27-8862747, Fax: +86-27-88663043.

Dr. Run Zhang, Email: r.zhang@uq.edu.au, Phone: +61 7 3346 3806, Fax: + 61 7 3346 3978

Graphical abstract

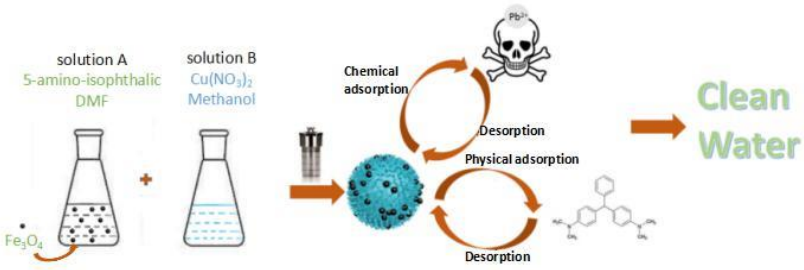

Abstract

We designed and synthesized a magnetic metal organic frameworks (MOFs) composite, Cu-MOFs/Fe_3O_4 as the adsorbent for removal of lead (Pb(II)) and malachite green (MG) in wastewater. This Cu-MOFs/Fe_3O_4 can be easily prepared by in-situ growth of Cu-MOFs with doping Fe_3O_4 nanoparticles. The prepared Cu-MOFs/Fe_3O_4 composite was well characterized by SEM, XRD, and FTIR spectra. The adsorption experiments found that Cu-MOFs/Fe_3O_4 can serve as adsorbent for removal of Pb(II) and MG simultaneously. The adsorption capacities were found to be 113.67mg/g for MG and 219.00 mg/g for Pb^{2+}, respectively, which are significantly higher than reported materials. Adsorption isotherm, kinetics and recyclability of Cu-MOFs/Fe_3O_4 for removal of Pb(II) and MG were then studied. Adsorption of Pb(II) and MG exhibited Freundlich adsorption isotherm model, with the adsorption kinetics of available second-order kinetic. Physical adsorption for MG and chemical adsorption for Pb(II) were confirmed by Dubinin-Radushkevich (D-R) isothermal adsorption model. The adsorption of Pb(II) and MG in real water samples were then studied. The Fe_3O_4/Cu-MOFs was found to be recyclable for removal of Pb(II) and MG, can be explored as the potential adsorbent for waste water treatment.

Keywords: Metal organic frameworks;magnetic composite;adsorption; malachite green;Lead;water treatment

1 Introduction

Environmental pollution, in particular water pollution have drawn considerable attention in recently years, because serious problems have been made to humans and other live organisms[1-3]. In addition to the efforts to reduce the discharging of pollutants, developing effective approaches to remove the existing pollutants, such as organic dyes, and heavy metals from contaminated water are essential to ensure the clear water supplying [4, 5]. Both organic dyes and heavy metals are normally existed in waste water, causing several problems for their removal simultaneously [6]. Therefore, it is desirable if the materials used for treatment can remove both dyes and heavy metals from the wastewater before it is discharged into the environment.

Malachite Green (MG) is a basic dye, being widely used in textile and dyestuff industries. Contamination of MG in water causes serious problems for human and animal health due to its poisonous, carcinogenic, mutagenic or respiratory effects being found at high concentration in water [7, 8]. It is well know that lead (Pb(II)) is a hypertoxic, biology accumulative and caustic heavy metal. Especially, this metal shows strong biological toxicities to human and other animals in the end of food chain [9, 10]. This metal is not degradable, can covert to other

chemical forms in live organisms after binding to biomolecules [11-13]. Thus, removal of these organic dyes and heavy metals will directly benefit to both environments and living creatures [14, 15].

Towards this end, a large number of approaches have been applied for removal of dyes from wastewater, such as adsorption, membrane-based separation, electro-coagulation, biochemical degradation and oxidative degradation [16-21]. Among them, adsorption technology has been widely recognized to be one of the most effective methods due to its high efficiency and ease of handling[22]. In particular, the adsorbents and other relevant materials can be recycled, significantly reduced the cost for the wastewater treatment. Traditional adsorbents, such as chitosan/natural zeolites, activated carbon, and silica microspheres, have been generally used in the water treatment by wastewater industries [23]. Those materials are normally applicable for the dyes or heavy metal pollution at low concentrations because their insufficient adsorption capacity.

The use of metal organic frameworks (MOFs) as the absorbent for removal of pollutants has attracted considerable interests in recent years due to its large surface area and adjustable pore size [24, 25]. These materials are also well known as the inorganic polymer that possess unique chemical and physical properties, being widely used in gas separation, photo-electro-catalysis, drug delivery, sensing, adsorption, and gas-storage [26-30]. Cu-MOFs is composed of oxygen, nitrogen, other organic ligands and copper ions from the self-assembly of the coordination polymer. In the preparation of Cu-MOFs, the arrangement of organic ligands and metal ions exhibits obvious direction, and different pore structures can be formed with different adsorption

properties, optical properties, and electromagnetic properties. As a result, Cu-MOFs has shown great potential and attractive prospects in modern material science field [25].

With specific ligands that can coordination with metal ions, MOFs can also be used for removal heavy metals. For example, it is well documented that N atoms from amino group can bind to heavy metal ions, such as Pb(II) through a dative bond [31, 32]. Therefore, amino group terminated Cu-MOFs is expected to be able to adsorption of Pb(II) in waste water in this contribution. In addition, the internal porous structure of amino Cu-MOFs allows adsorption of MG, providing a material for removal both heavy metals and organic dyes simultaneously.

It has been reported that the stability of MOFs can be significantly enhanced in aqueous solution with support by a nano-/micro-composite [33]. In addition to the enhancement of stability, the hybrid composite can also be designed to facilitate the recycling processes for MOFs after adsorption of organic dyes and heavy metals.[34] To this purpose, the magnetic nanoparticle, Fe_3O_4, could be a good choice as the separation in the water samples can be achieved simply by an external magnetic field [35, 36]. Therefore, preparing magnetic composites combination MOFs with magnetic nanoparticles has significant superiorities in adsorption and separation of pollution.

In this work, a new Cu-MOFs/Fe_3O_4 composite was designed and synthesized for removal Pb(II) and MG simultaneously (Scheme 1). Integrating of the porous structure of Cu-MOFs with the magnetic Fe_3O_4 particles, Cu-MOFs/Fe_3O_4 composite was able to be used as an effective adsorbent for MG and Pb(II) removal. Recycling of Cu-MOFs/Fe_3O_4 composite can also be achieved by an external magnet. The adsorption properties for MG and Pb^{2+} of Cu-

MOFs/Fe_3O_4 composite were discussed, and the kinetics, thermodynamics and adsorption isotherm were further studied. The feasibility of Cu-MOFs/Fe_3O_4 composite as adsorbent for removal of MG and Pb(II) in mixed wastewater samples was finally evaluated.

2 Experimental

2.1 Chemicals and materials

Copper nitrate ($Cu(NO_3)_2$), N, N-dimethyformamide (DMF), sodium acetate, ethanol (EtOH), ethylene glycol (EG) were obtained from Sinopharm Group Chemical Reagent Company. Malachite Green (92.7 mg L^{-1}), $FeCl_3 \cdot 6H_2O$, 5-amino-isophthalic acid, lead nitrate ($Pb(NO_3)_2$) were purchased from Aladdin Reagent Company (Shanghai). Fresh double distilled water was used throughout the experiment. MG solution with different concentration was prepared by diluting of stock MG solution with water, and stock solution of Pb^{2+} (1000mg L^{-1}) was prepared by dissolving $Pb(NO_3)_2$ in water.

2.2 Characterization

The chemical composition of Fe_3O_4 and Cu-MOFs/Fe_3O_4 composite were determined by D/max-IIIC X-ray diffractometer (Shimadzu, Japan). The Fourier transform infrared spectroscopy was measured by a FTIR spectrometer (Perkin Elmer, USA). Scanning electron microscope (SEM) images were obtained using a JSM6510LV scanning electron microscope (JEOL, Japan). N_2 adsorption-desorption analysis was performed on an Accelerated Surface Area and Porosimetry System ASAP2020 (Micromeritics, American). The surface area was estimated using the BET equation, and the pore size distribution was determined by the BJH

model.UV-vis absorption spectra were measured with a Lambda 900 UV/VIS/NIR spectrophotometer (Perkin Elmer, USA). Inductively coupled plasma-mass spectra (ICP-MS, Perkin Elmer, USA) was employed to measure the concentration of Pb(II).

2.3 Synthesis of Cu-MOFs/Fe_3O_4 composite

2.3.1 Synthesis of Fe_3O_4 nanoparticle

The magnetic Fe_3O_4 nanoparticles were synthetized by following reported method [37]. Briefly, 1.73g $FeCl_3 \cdot 6H_2O$ and 2.31g sodium acetate were dissolved in 35 mL ethylene glycol (EG) with stirring for 0.5 h. The mixture was then transferred into a Teflon-lined autoclave, sealed and heated at 200 ^oC for 8 h. The systems were then allowed to naturally cool to room temperature. The final products collected by centrifugation, washed with ethanol and water for several times to remove any possible remnants, and then dried under vacuum at 60 ^oC for 8 hours to obtain powder Fe_3O_4 nanoparticles.

2.3.2 Synthesis of Cu-MOFs and Cu-MOFs/Fe_3O_4 composite

For synthesis of Cu-MOFs, 0.4 g 5-amino-isophthalic acid solution in 20 mL DMF was added into a EtOH solution (15 mL) containing 1.2 g $Cu(NO_3)_2$. The mixture was then transferred into a Teflon-lined autoclave, sealed and heated at 120 ^oC for 12 h. The formed sediment was collected by filtration, and washed with ethanol and water for three times. For preparation of Cu-MOFs/Fe_3O_4 composite, 0.15 g Fe_3O_4 nanoparticles were added into 20 mL DMF containing 0.4 g 5-amino-isophthalic acid with stirring. After stirring at R. T. for 10 min, 1.2 g $Cu(NO_3)_2$ in 15 mL EtOH was added. The mixture was then transferred into Teflon-lined

autoclave for heating at 120 ºC for 12 h. The products were then collected, and washed with EtOH-H_2O for several times to obtain Cu-MOFs/Fe_3O_4 composite.

2.4 Adsorption experiments

For adsorption of MG, the Cu-MOFs/Fe_3O_4 composite (50.0 mg) was added to 5 mL MG solution at different concentration, and the mixture was shaken for certain time (5-60 min) at 25 ºC, 35 ºC, 45 ºC, separately. The solution was then placed closely to a magnet for 5 min, and then the water solution was removed. The residual MG was then analyzed using UV spectrometer at the wavelength of 620 nm. For investigation the dynamic adsorption, the concentration of MG in water solution was also measured at the different time point.

For adsorption of Pb(II), the Cu-MOFs/Fe_3O_4 composite (50.0 mg) was added into a water solution containing different concentration of Pb^{2+}. Shaking at 5 ºC, 35 ºC, 45 ºC, the concentration of Pb^{2+} was measured at each 10 min until the saturated adsorption reached. Then, the concentration of Pb^{2+} in Cu-MOFs/Fe_3O_4 composite was measured by ICP-MS.

2.5 Desorption experiments

For recovery of Cu-MOFs/Fe_3O_4 composite, the used composite was treated with acetone, followed by EDTA. The used Cu-MOFs/Fe_3O_4 composite was mixed with acetone under stirring for 30 min. After repeating for three time, the Cu-MOFs/Fe_3O_4 composite was dried at R. T. for 5 min, and then placed into a solution contains 0.1 M EDTA. Stirring the mixture for 3 h, washing with water for three times before reuse the regenerated Cu-MOFs/Fe_3O_4 composite.

3 Results and discussion

3.1 Characterization of Cu-MOFs/Fe_3O_4 composite

The morphology of the Fe_3O_4 nanoparticles, Cu-MOFs, and Cu-MOFs/Fe_3O_4 composite were characterized by scanning electron microscopy (SEM). As shown in Fig. 1, uniform size and shapes of Fe_3O_4 nanoparticles were obtained with an average diameter of 400 nm. The Cu-MOFs exhibited a spherical flower-like structure before coating of Fe_3O_4 nanoparticles. No significant changes on the shapes of Cu-MOFs/Fe_3O_4 composite was noticed after growth of Fe_3O_4 nanoparticles, but obviously the Fe_3O_4 nanoparticles have been embedded within Cu-MOFs shown in Fig. 1d.

The formation of Cu-MOFs/Fe_3O_4 composite was further confirmed by powder XRD measure of Fe_3O_4 nanoparticles, Cu-MOFs, and Cu-MOFs/Fe_3O_4 composite. As shown in Fig. 2, the diffraction peaks at 2θ = 18.94 °, 30.16 °, 35.54 °, 43.07 °, 53.6 °, 57.1 ° and 62.70 ° were obtained, which are in consistent with the diffraction plate PDF#99-0073 at (300), (220), (311), (400), (411), (440). Sharp diffraction of Cu-MOFs was also obtained, suggesting a well crystal structure obtained. The diffraction peaks of Cu-MOFs/Fe_3O_4 composite were well matched with Fe_3O_4 and Cu-MOFs, corroborating the presence of Fe_3O_4 nanoparticles in the composite.

FTIR spectra of the Fe_3O_4, Cu-MOF and Fe_3O_4/Cu-MOFs were presented in Fig. 3. The peak at 3500 cm^{-1} of Cu-MOFs is assigned to amino group termination. The bending vibration of N-H from 5-amino-isophthalic acid can be supported by the peaks observed at 1500~1650 cm^{-1}. The peaks at 1230-1030 cm^{-1}, can be assigned to the stretching vibration peak of C-N. These

peaks were also clearly observed from Fe_3O_4/Cu-MOFs, suggesting the formation of Cu-MOFs/Fe_3O_4 composite. For the spectra of Fe_3O_4 nanoparticles, the peak at 588 cm^{-1} can be assigned to Fe-O vibration. The shift of this peak may be caused by the interaction between Fe_3O_4 and Cu-MOFs.

3.2 The adsorption of Cu-MOFs/Fe_3O_4 composite towards MG and Pb(II)

Fig. 4 shows the N_2 adsorption – desorption isotherms and pore size distributions of Cu-MOFs/Fe_3O_4. The Curves show IV type isotherm, which means Cu-MOFs/Fe_3O_4 is with mesoporous structure. Based on the pore size distribution curves, obvious mesoporous distribution can be observed in 3.5 nm, 4 nm and 8.5 nm. The BET surface area and pore volume is 35.4 $m^2 \cdot g^{-1}$.

The adsorption properties of Cu-MOFs/Fe_3O_4 composite towards MG and Pb^{2+} were then investigated and the results showed in Fig. 5. Using Cu-MOFs/Fe_3O_4 composite, the removal efficiency for MG was found to be 90 %. The removal efficiency was increased with higher concentration of MG. As shown in Fig. 5b, the removal efficiency for Pb(II) was measured to be 96 % at low concentration at concentration less than 10 mg/L. Upon increasing the concentration of Pb(II), the removal efficiency was gradually decreased. Nevertheless, 80% Pb^{2+} was removed at the concentration of 1000 mg/L, suggesting high efficiency of Cu-MOFs/Fe_3O_4 composite for Pb(II) removal.

The difference of Cu-MOFs/Fe_3O_4 composite for removal of MG and Pb(II) may be attributed to the adsorption processes. In contrast with the physical adsorption for MG, chemical adsorption of Pb(II) is mainly dominated by the coordination of Pb^{2+} with amino from Cu-

MOFs. The removal efficiency could be decreased when the N-Pb bond was saturated.

The maximum adsorption capacities for MG and Pb^{2+} were then calculated. As shown in Table 1, higher adsorption capacity of Cu-MOFs/Fe_3O_4 composite for MG and Pb(II) removal was obtained in this work.

In order to undersand the adsorpiton ability, tradtional adsorbents are compared, and the result is shown in Fig.6.

It is clear that, the removal efficiency of Cu-MOFs/Fe_3O_4 for MG is a bit better than that of zeolite and activated carbon (Fig. 6 a), the reason may be the physical adsorption for dyes results from the pore size. Even if the surface area of Cu-MOFs/Fe_3O_4 is not large, but the pore size is with mesoporous structure. The excellent adsorption for MG is due to the appropriate matching of the channel diameter and the dye molecular width[42,43]. Therefore, it can adsorb MG with relative adsorption capacity.

Fig.6 b shows that the removal efficiency for Pb^{2+} is absolutedly better than that of zeolite and activated carbon. It can further proves that the adsorption is chemical adsorption which is dominated by the coordination of Pb^{2+} with amino from Cu-MOFs. From the comparison, the Cu-MOFs/Fe_3O_4 can be proved as an adsorbent for mixed-wastewater treatment.

To examine the superparamagnetic nature of Cu-MOFs/Fe_3O_4 composite, we placed the Cu-MOFs/Fe_3O_4 composite close to an external magnet. As shown in Fig. 7, the Cu-MOFs/Fe_3O_4 composite can be easily separated from the solution within a few seconds. This superparamagnetic nature was not changed after adsorption of MG and Pb(II), indicating the

capability in magnetic recovery of Cu-MOFs/Fe_3O_4 composite after treatment.

3.3 Adsorption isotherms for MG and Pb^{2+}

Freundlich model was then selected to study the adsorption isotherm of Cu-MOFs/Fe_3O_4 composite for removal of MG and Pb(II). The Freundlich equation can be described as:

$$Q_e = K_F C e^{1/n} \qquad (1)$$

where K_F and 1/n were the Freundlich constant related to adsorption capacity and intensity, respectively. Two linear plots, $\ln Q_e$ aganist $\ln C_e$ was obtained for adsorption of MG and Pb(II), respectively. It was found that the removal of MG and Pb(II) are following Freundlich adsorption isotherm model.

3.4 Dubinin-Radushkevich (D-R) isotherm

Dubinin-Radushkevich (D-R) isotherm adsorption process was then investigated to understand the principle of adsorption, *i. e.*, chemical adsorption and/or physical adsorption processes [44, 45]. The Dubinin-Radushkevich (D-R) isothermal adsorption model can be described as:

$$\ln Q_e = \ln Q_m - B_d[RT\ln(1 + 1/C_e)]^2 \qquad (2)$$

$$E = 1/(2B_d)^{1/2} \qquad (3)$$

where Q_e was the equilibrium adsorption capacity of MG and Pb^{2+} on the Fe_3O_4/Cu-MOFs (mol/g), respectively; B_d (mol^2/J^2) was the activity factor correlated with mean free energy of adsorption, R was the ideal gas constant (8.314 $J \cdot mol^{-1} \cdot K^{-1}$), T (K) was the Kelvin temperature, and E (kJ/mol) was the average free energy of adsorption. Chemical adsorption

normally showed the energy E at the range of 8-16 KJ/mol, while physical adsorption was happened when E is less than 8.

Linear plots between $\ln Q_e$ and $RT\ln(1+1/C_e)$ at different temperatures were shown in Fig. 9. The D-R constants were estimated using separate intercept and slope of linear plots. For the adsorption process for MG, E was calculated to be 1.81, 5.83 and 9.47 KJ/mol at different temperatures (a, b and c), respectively. This indicated that the adsorption for MG was mainly physical adsorption at low temperature. With the increasing temperature, chemical adsorption was involved besides the physical adsorption. For the adsorption process for Pb^{2+}, E was determined to be 10.64, 12.13 and 13.88 KJ/mol at different temperatures (d, e and f), which are all located in the level of 8-16 KJ/mol, suggesting the removal of Pb^{2+} was mainly dominated by chemical adsorption process.

3.5 Kinetics for the adsorption of MG and Pb^{2+}

To study the kinetics for adsorption of MG and Pb^{2+}, time-dependent adsorptions capacity was then measured at different temperature. The applicability of the pseudo-first-order kinetic model and pseudo-second-order kinetic model were tested by fitting the experimental data. The results showed that the adsorption of MG and Pb^{2+} are following pseudo-second-order kinetic model (Fig. 10). The thermodynamic equilibrium constant (K) and the free energy change (ΔG) were also calculated on basis of the adsorption equilibrium at different temperature, and the results were shown in Table 2. The data of negative free energy (ΔG) and the positive enthalpy change (ΔH) suggested that the adsorption for MG and Pb^{2+} were spontaneous and endothermic processes.

3.6 Recycle of Cu-MOFs/Fe_3O_4 composite

Desorption experiments were then carried out to evaluate the regeneration of Cu-MOFs/Fe_3O_4 composite after MG and Pb^{2+} adsorption. Considering the different adsorption processes, two different eluents, acetone and EDTA were selected to removal of MG and Pb^{2+}, separately. As shown in Fig.11. it was found that the MG removal efficiency was 90% after recycling Cu-MOFs/Fe_3O_4 composite for five times. Although the strong chemical adsorption for Pb^{2+}, over 85% removal efficiency was obtained after recycling the Cu-MOFs/Fe_3O_4 composite for three time. However, the removal efficiency reduced to 50% if further adsorption performed. These results demonstrated that the Cu-MOFs/Fe_3O_4 composite can be recycled for MG and Pb^{2+} adsorption, which is extremely important for a adsorbent to be potential used in future water treatment industry.

2.6 Removal of MG and Pb^{2+} in real water sample

To evaluate the practical application of Cu-MOFs/Fe_3O_4 composite, adsorption of MG and Pb^{2+} in was then evaluated in a real water sample collected from Yangtze River locally. The water was firstly filtered to remove big solid particles, sand, and live organisms. The water samples were spiked with both MG and Pb^{2+} at certain concentration. Cu-MOFs/Fe_3O_4 composite was then added into the samples with shaking. The Cu-MOFs/Fe_3O_4 composite was further collected by a magnet, and the samples were then analyzed to obtain the removal efficiency.

As shown in Table 3, the removal efficiencies for MG and Pb^{2+} were found to be over 89.92% and 86.75%, respectively. The removal efficiency for both MG and Pb^{2+} are concentration independent. The results demonstrated that Cu-MOFs/Fe_3O_4 composite can be used for

adsorption of MG and Pb^{2+} in real water sample with high removal efficiency.

4 Conclusions

In this work, a recyclable Cu-MOFs/Fe_3O_4 composite was designed and synthesized for adsorption of organic dyes (MG) and heavy metals (Pb^{2+}). The prepared Cu-MOFs/Fe_3O_4 composite was well characterized by FTIR, XRD, and SEM. Removal of MG and Pb^{2+} in water sample can be easily achieved by gentle shaking and magnet separation. Removal efficiency was further studied, and the results showed over 90% adsorption efficiency for both MG and Pb^{2+} removal. The maximum adsorption capacity for Pb^{2+} and MG were determined to be 219.00 mg/g and 113.67mg/g, respectively, which is much higher than the reported methods. Studies on adsorption mechanisms demonstrated the removal of MG was mainly dominated by physical adsorption, and removal of Pb^{2+} was based on chemical binding with N of the ligands. Becuase the physical adsorption for dyes and chemical adsorption for metal ions, the Cu-MOFs/Fe_3O_4 composite can be potentially applied to real polluted water with the existing pollutants, such as organic dyes, and heavy metals from contaminated water. The Cu-MOFs/Fe_3O_4 composite was found to be recyclable, can be further used for five times after washing with acetone and EDTA solution. The application of this Cu-MOFs/Fe_3O_4 composite for removal of MG and Pb^{2+} in practical water samples were then demonstrated. The successful development of this Cu-MOFs/Fe_3O_4 composite not only provides an effective method for removal of MG and Pb^{2+} in water samples, but also extend the extend the industrial application of inorganic materials.

Acknowledgement

This work was supported by Natural Science Foundation of Hubei province (No.2017CFB530) and Wuhan Morning Light Plan of Youth Science and Technology (No.2017050304010282). The authors are grateful for financial aid from the National Natural Science Foundation of China (Grant No. 51302071, No. 21601076) and the Australian Research Council (ARC DE170100092).

References

[1] L. Sun, S. Hu, H. Sun, H. Guo, H. Zhu, M. Liu, H. Sun, Malachite green adsorption onto Fe_3O_4@SiO_2-NH_2: isotherms, kinetic and process optimization, RSC Adv. 5 (2015) 11837-11844.

[2] H.H. Hammud, A. Shmait, N. Hourani, Removal of Malachite Green from water using hydrothermally carbonized pine needles, RSC Adv. 5 (2015) 7909-7920.

[3] M. Babazadeh, R. Hosseinzadeh-Khanmiri, J. Abolhasani, E. Ghorbani-Kalhor, A. Hassanpour, Solid phase extraction of heavy metal ions from agricultural samples with the aid of a novel functionalized magnetic metal–organic framework, RSC Adv. 5 (2015) 19884-19892.

[4] A.S. Sartape, A.M. Mandhare, V.V. Jadhav, P.D. Raut, M.A. Anuse, S.S. Kolekar, Removal of malachite green dye from aqueous solution with adsorption technique using Limonia acidissima (wood apple) shell as low cost adsorbent, Arabian Journal of Chemistry (2013).

[5] Z.A. Al Othman, M.A. Habila, A. Hashem, Removal of zinc(II) from aqueous solutions using modified agricultural wastes: kinetics and equilibrium studies, Arabian Journal of Geosciences 6 (2012) 4245-4255.

[6] E.A. Dil, M. Ghaedi, A. Asfaram, The performance of nanorods material as adsorbent for removal of azo dyes and heavy metal ions: Application of ultrasound wave, optimization and modeling, Ultrasonics sonochemistry 34 (2017) 792-802.

[7] H. Zhang, F. Zhang, Q. Huang, Highly effective removal of malachite green from aqueous solution by hydrochar derived from phycocyanin-extracted algal bloom residues through hydrothermal carbonization, RSC Adv. 7 (2017) 5790-5799.

[8] B. Ekka, S.R. Nayak, P. Dash, R.K. Patel, Removal of malachite green dye from aqueous

solution using mesoporous silica synthesized from 1-octyl-3-methylimidazolium chloride ionic liquid, 1249 (2016) 020011.

[9] Y. Zhang, Y. Li, X. Li, L. Yang, X. Bai, Z. Ye, L. Zhou, L. Wang, Selective removal for Pb^{2+} in aqueous environment by using novel macroreticular PVA beads, Journal of hazardous materials 181 (2010) 898-907.

[10] D.H.K. Reddy, S.-M. Lee, Three-Dimensional Porous Spinel Ferrite as an Adsorbent for Pb(II) Removal from Aqueous Solutions, Industrial & Engineering Chemistry Research 52 (2013) 15789-15800.

[11] X. Luo, L. Ding, J. Luo, Adsorptive Removal of Pb(II) Ions from Aqueous Samples with Amino-Functionalization of Metal–Organic Frameworks MIL-101(Cr), Journal of Chemical & Engineering Data 60 (2015) 1732-1743.

[12] J. Zhang, S. Zhai, S. Li, Z. Xiao, Y. Song, Q. An, G. Tian, Pb(II) removal of Fe_3O_4@SiO_2–NH_2 core–shell nanomaterials prepared via a controllable sol–gel process, Chemical Engineering Journal 215-216 (2013) 461-471.

[13] A. Tadjarodi, A. Abbaszadeh, M. Taghizadeh, N. Shekari, A.A. Asgharinezhad, Solid phase extraction of Cd(II) and Pb(II) ions based on a novel functionalized Fe_3O_4@ SiO_2 core-shell nanoparticles with the aid of multivariate optimization methodology, Materials science & engineering. C, Materials for biological applications 49 (2015) 416-421.

[14] N. Yin, K. Wang, L. Wang, Z. Li, Amino-functionalized MOFs combining ceramic membrane ultrafiltration for Pb (II) removal, Chemical Engineering Journal 306 (2016) 619-628.

[15] Y. Tan, M. Chen, Y. Hao, High efficient removal of Pb (II) by amino-functionalized Fe_3O_4

magnetic nano-particles, Chemical Engineering Journal 191 (2012) 104-111.

[16] M. El-Bouraie, Removal of the Malachite Green (MG) Dye From Textile Industrial Wastewater Using the Polyurethane Foam Functionalized with Salicylate, Journal of Dispersion Science and Technology 36 (2014) 1228-1236.

[17] M. Yusuf, M.A. Khan, M. Otero, E.C. Abdullah, M. Hosomi, A. Terada, S. Riya, Synthesis of CTAB intercalated graphene and its application for the adsorption of AR265 and AO7 dyes from water, Journal of colloid and interface science 493 (2017) 51-61.

[18] A.J. Sami, M. Khalid, S. Iqbal, M. Afzal, A.R. Shakoori, Synthesis and Application of Chitosan-Starch Based Nanocomposite in Wastewater Treatment for the Removal of Anionic Commercial Dyes, Pakistan Journal of Zoology 49 (2016) 21-26.

[19] A. Omidvar, B. Jaleh, M. Nasrollahzadeh, Preparation of the GO/Pd nanocomposite and its application for the degradation of organic dyes in water, Journal of colloid and interface science 496 (2017) 44-50.

[20] H. Jayasantha Kumari, P. Krishnamoorthy, T.K. Arumugam, S. Radhakrishnan, D. Vasudevan, An efficient removal of crystal violet dye from waste water by adsorption onto TLAC/Chitosan composite: A novel low cost adsorbent, International journal of biological macromolecules 96 (2017) 324-333.

[21] K.C. de Souza, M.L.P. Antunes, S.J. Couperthwaite, F.T. da Conceição, T.R. de Barros, R. Frost, Adsorption of reactive dye on seawater-neutralised bauxite refinery residue, Journal of colloid and interface science 396 (2013) 210-214.

[22] L. Li, X.L. Liu, H.Y. Geng, B. Hu, G.W. Song, Z.S. Xu, A MOF/graphite oxide hybrid (MOF: HKUST-1) material for the adsorption of methylene blue from aqueous solution,

Journal of Materials Chemistry A 1 (2013) 10292.

[23] M.A. Habila, Z.A. Alothman, A.M. El-Toni, J.P. Labis, X. Li, F. Zhang, M. Soylak, Mercaptobenzothiazole-functionalized magnetic carbon nanospheres of type Fe_3O_4@SiO_2@C for the preconcentration of nickel, copper and lead prior to their determination by ICP-MS, Microchimica Acta 183 (2016) 2377-2384.

[24] K.-D. Zhang, F.-C. Tsai, N. Ma, Y. Xia, H.-L. Liu, X.-Q. Zhan, X.-Y. Yu, X.-Z. Zeng, T. Jiang, D. Shi, C.-J. Chang, Adsorption Behavior of High Stable Zr-Based MOFs for the Removal of Acid Organic Dye from Water, Materials 10 (2017) 205.

[25] L. Li, X.L. Liu, M. Gao, W. Hong, G.Z. Liu, L. Fan, B. Hu, Q.H. Xia, L. Liu, G.W. Song, Z.S. Xu, The adsorption on magnetic hybrid Fe_3O_4/HKUST-1/GO of methylene blue from water solution, J. Mater. Chem. A 2 (2014) 1795-1801.

[26] M. Roushani, Z. Saedi, T. Musa beygi, Anionic dyes removal from aqueous solution using TMU-16 and TMU-16-NH_2 as isoreticular nanoporous metal organic frameworks, Journal of the Taiwan Institute of Chemical Engineers 66 (2016) 164-171.

[27] C. Pettinari, F. Marchetti, N. Mosca, G. Tosi, A. Drozdov, Application of metal − organic frameworks, Polymer International 66 (2017) 731-744.

[28] J.R. Li, Y. Ma, M.C. McCarthy, J. Sculley, J. Yu, H.-K. Jeong, P.B. Balbuena, H.-C. Zhou, Carbon dioxide capture-related gas adsorption and separation in metal-organic frameworks, Coordination Chemistry Reviews 255 (2011) 1791-1823.

[29] K. Sun, L. Li, X. Yu, L. Liu, Q. Meng, F. Wang, R. Zhang, Functionalization of mixed ligand metal-organic frameworks as the transport vehicles for drugs, Journal of colloid and interface science 486 (2017) 128-135.

[30] S. Liu, L. Sun, F. Xu, J. Zhang, C. Jiao, F. Li, Z. Li, S. Wang, Z. Wang, X. Jiang, H. Zhou, L. Yang, C. Schick, Nanosized Cu-MOFs induced by graphene oxide and enhanced gas storage capacity, Energy & Environmental Science 6 (2013) 818.

[31] B. Arstad, H. Fjellvåg, K.O. Kongshaug, O. Swang, R. Blom, Amine functionalised metal organic frameworks (MOFs) as adsorbents for carbon dioxide, Adsorption 14 (2008) 755-762.

[32] S.K. Henninger, H.A. Habib, C. Janiak, MOFs as adsorbents for low temperature heating and cooling applications, Journal of the American Chemical Society 131 (2009) 2776-2777.

[33] T.J. Bandosz, C. Petit, MOF/graphite oxide hybrid materials: exploring the new concept of adsorbents and catalysts, Adsorption 17 (2010) 5-16.

[34] W. Xuan, C. Zhu, Y. Liu, Y. Cui, Mesoporous metal-organic framework materials, Chemical Society reviews 41 (2012) 1677-1695.

[35] M.E. Mahmoud, M.S. Abdelwahab, E.M. Fathallah, Design of novel nano-sorbents based on nano-magnetic iron oxide–bound-nano-silicon oxide–immobilized-triethylenetetramine for implementation in water treatment of heavy metals, Chemical Engineering Journal 223 (2013) 318-327.

[36] Z. Qiang, X. Bao, W. Ben, MCM-48 modified magnetic mesoporous nanocomposite as an attractive adsorbent for the removal of sulfamethazine from water, Water research 47 (2013) 4107-4114.

[37] X. Qiu, N. Li, S. Yang, D. Chen, Q. Xu, H. Li, J. Lu, A new magnetic nanocomposite for selective detection and removal of trace copper ions from water, J. Mater. Chem. A 3 (2015) 1265-1271.

[38] S. Rajput, L.P. Singh, C.U. Pittman, Jr., D. Mohan, Lead (Pb^{2+}) and copper (Cu^{2+})

remediation from water using superparamagnetic maghemite (gamma-Fe_2O_3) nanoparticles synthesized by Flame Spray Pyrolysis (FSP), Journal of colloid and interface science 492 (2017) 176-190.

[39] Y. Liu, R. Fu, Y. Sun, X. Zhou, S.A. Baig, X. Xu, Multifunctional nanocomposites Fe_3O_4@SiO_2-EDTA for Pb(II) and Cu(II) removal from aqueous solutions, Applied Surface Science 369 (2016) 267-276.

[40] S. Banerjee, G.C. Sharma, R.K. Gautam, M.C. Chattopadhyaya, S.N. Upadhyay, Y.C. Sharma, Removal of Malachite Green, a hazardous dye from aqueous solutions using Avena sativa (oat) hull as a potential adsorbent, Journal of Molecular Liquids 213 (2016) 162-172.

[41] L. Tian, J. Zhang, H. Shi, N. Li, Q. Ping, Adsorption of Malachite Green by Diatomite: Equilibrium Isotherms and Kinetic Studies, Journal of Dispersion Science and Technology 37 (2015) 1059-1066.

[42]Y. Dong, H. M. Lin , F. Y. Qu, Synthesis of ferromagnetic ordered mesoporous carbons for bulky dye molecules adsorption, Chemical Engineering Journal, 193-194 (2012) 169-177.

[43] R. Marguta, S. J. Khatib, J. M. Guil, E. Lomba, E. G. Noya, J. A. Perdig´on-Mel´on and S. Valencia, Molecular simulation and adsorption studies of n -hexane in ZSM-11 zeolites, Microporous Mesoporous Matererials, 142(2011) 258-267.

[44] M.H. Dehghani, M. Ghadermazi, A. Bhatnagar, P. Sadighara, G. Jahed-Khaniki, B. Heibati, G. McKay, Adsorptive removal of endocrine disrupting bisphenol A from aqueous solution using chitosan, Journal of Environmental Chemical Engineering 4 (2016) 2647-2655.

[45] F. Nekouei, S. Nekouei, I. Tyagi, V.K. Gupta, Kinetic, thermodynamic and isotherm studies for acid blue 129 removal from liquids using copper oxide nanoparticle-modified

activated carbon as a novel adsorbent, Journal of Molecular Liquids 201 (2015) 124-133.

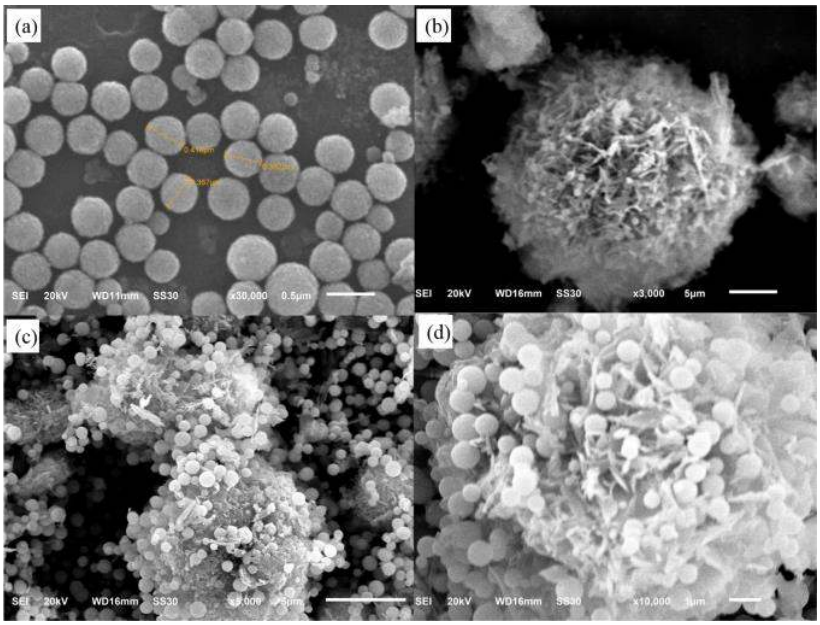

Fig. 1 SEM images of Fe_3O_4 nanoparticles (a), Cu-MOFs (b), and Cu-MOFs/Fe_3O_4 composite (c, d).

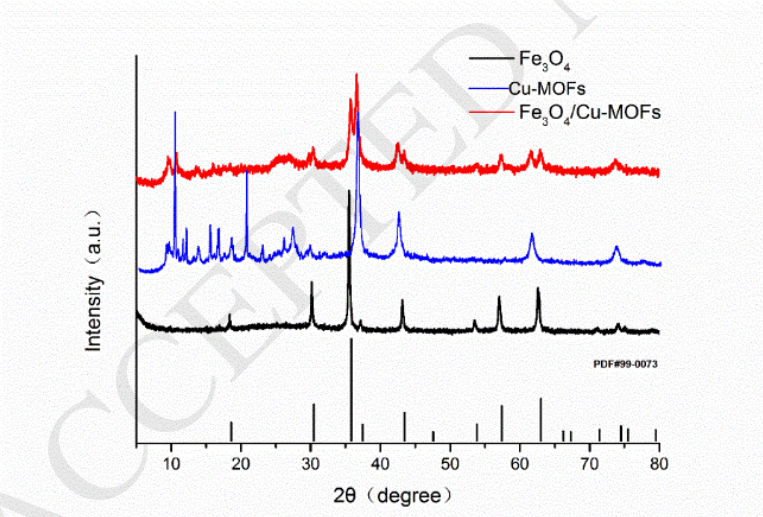

Fig. 2 XRD patterns

Fig. 3 FT-IR spectra of Fe_3O_4 nanoparticles, Cu-MOFs, and Cu-MOFs/Fe_3O_4 composite.

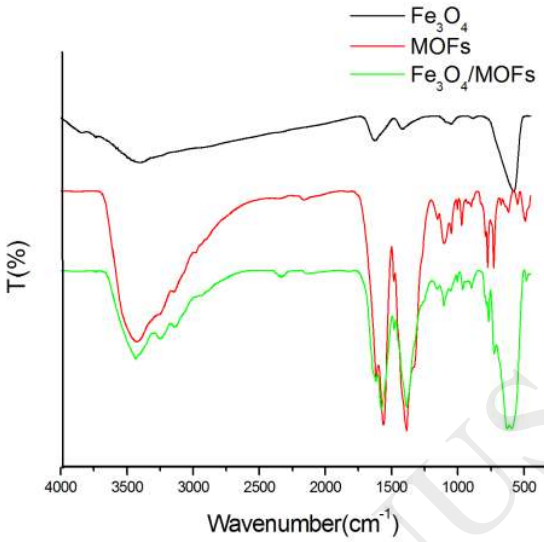

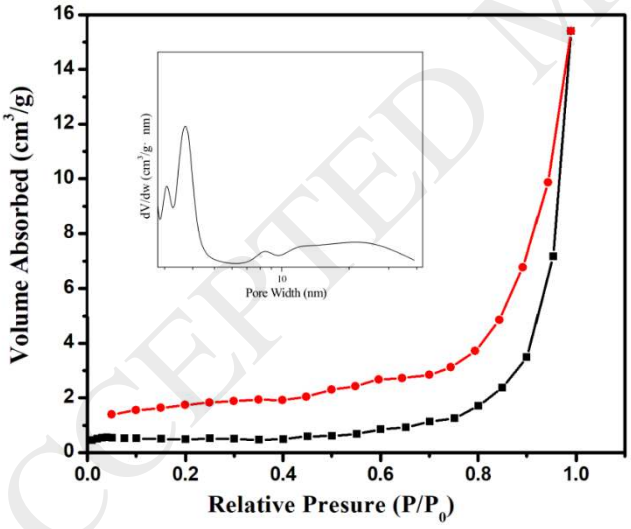

Fig. 4 N_2 adsorption–desorption isotherm and pore diameter distribution profile (insert)

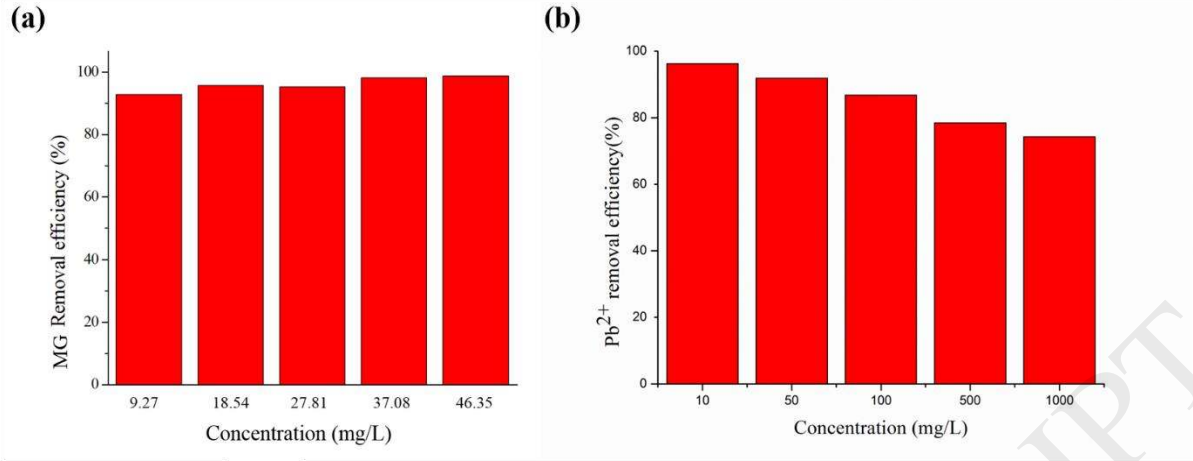

Fig. 5 The adsorption capability of Cu-MOFs/Fe_3O_4 composite towards MG (a) and Pb^{2+} (b) at different concentration.

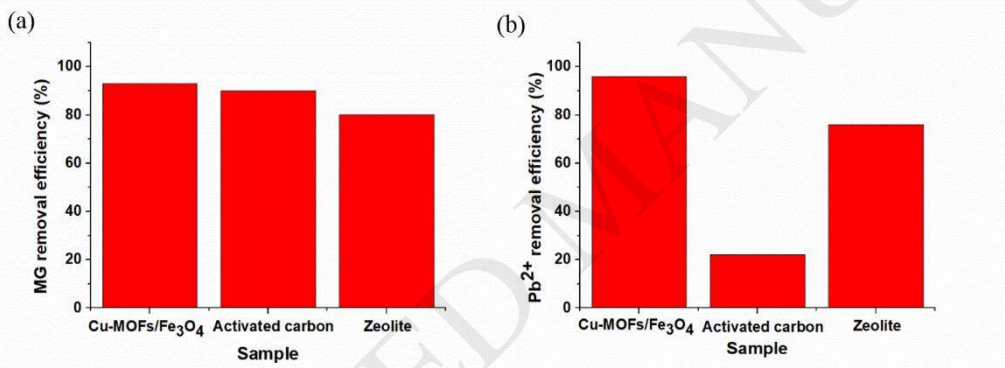

Fig.6 Adsorption for MG (a) and Pb^{2+} on different adsorbens

Fig. 7 Photographs demonstrating the magnetic separation of the Cu-MOFs/Fe_3O_4 composite before (a) and after (b) adsorption of MG and Pb(II).

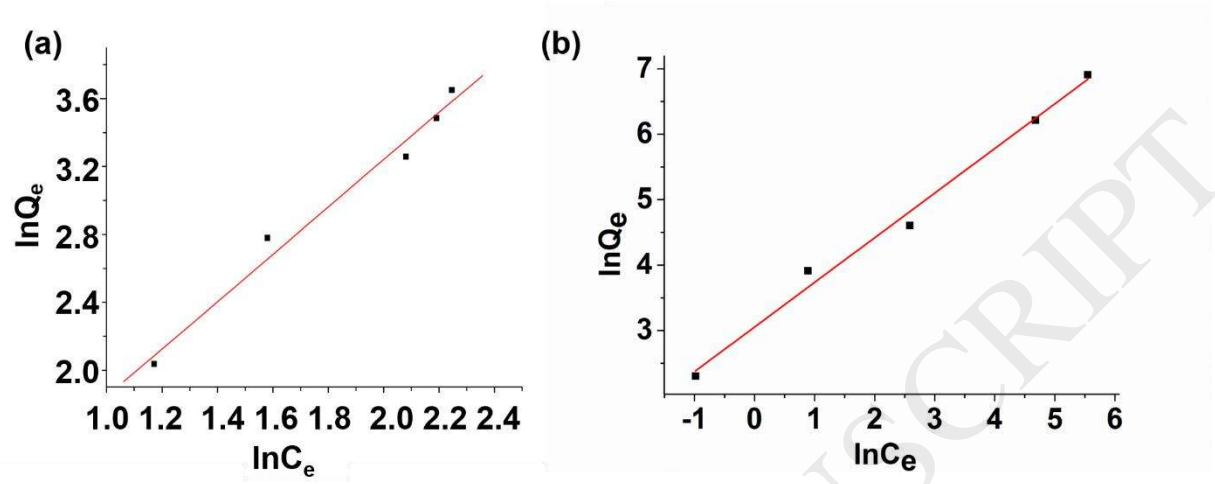

Fig. 8 Freundlich isothermal model of Cu-MOFs/Fe_3O_4 composite for adsorption of MG and Pb^{2+}.

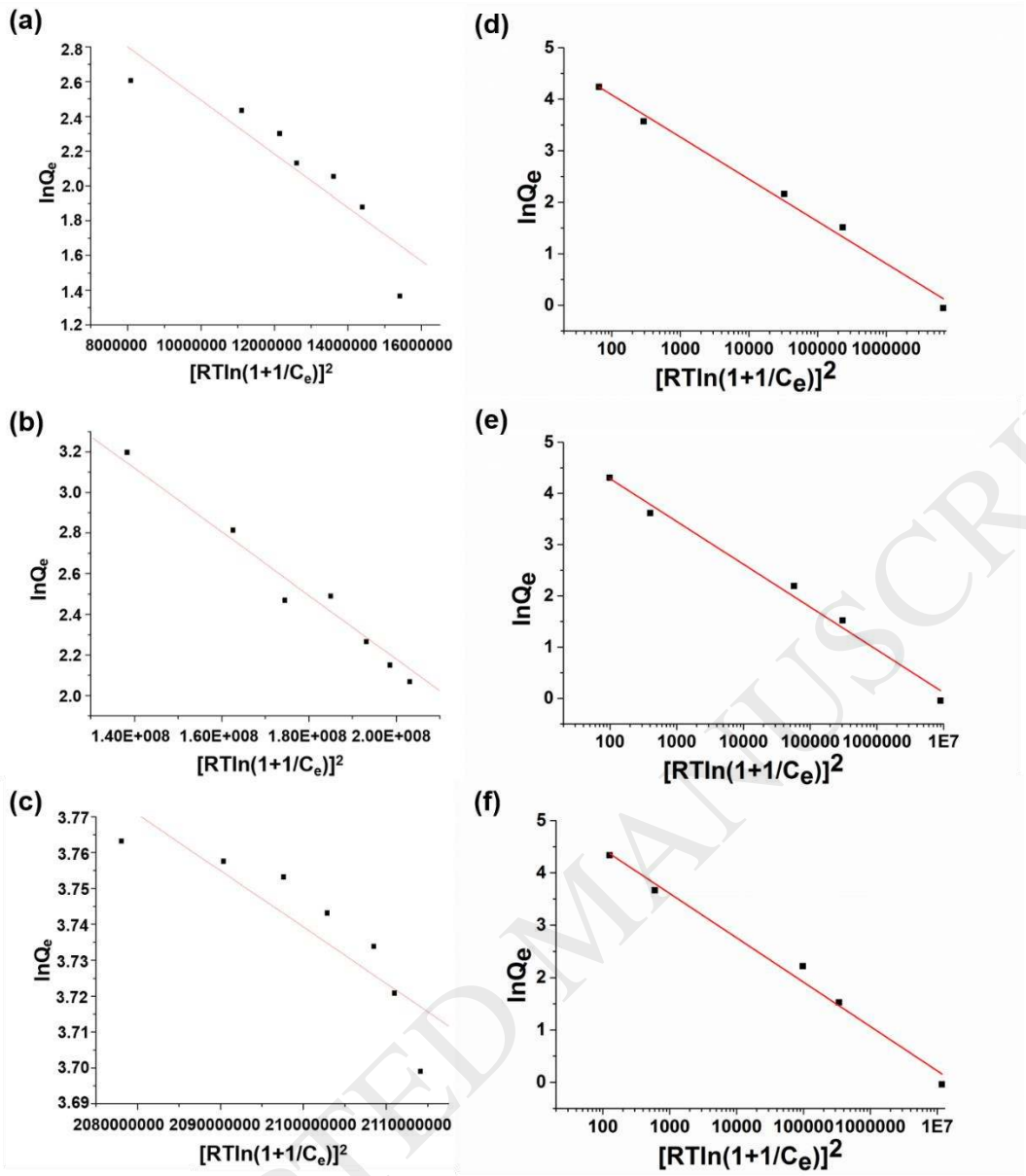

Fig.9 Dubinin-Radushkevich (D-R) isothermal adsorption model of Fe_3O_4/Cu-MOFs for removal of MG at 298 K (a), 308 K (b), and 318 K (c); Pb^{2+} at 298 K (d), 308 K (e), and 318 K (f).

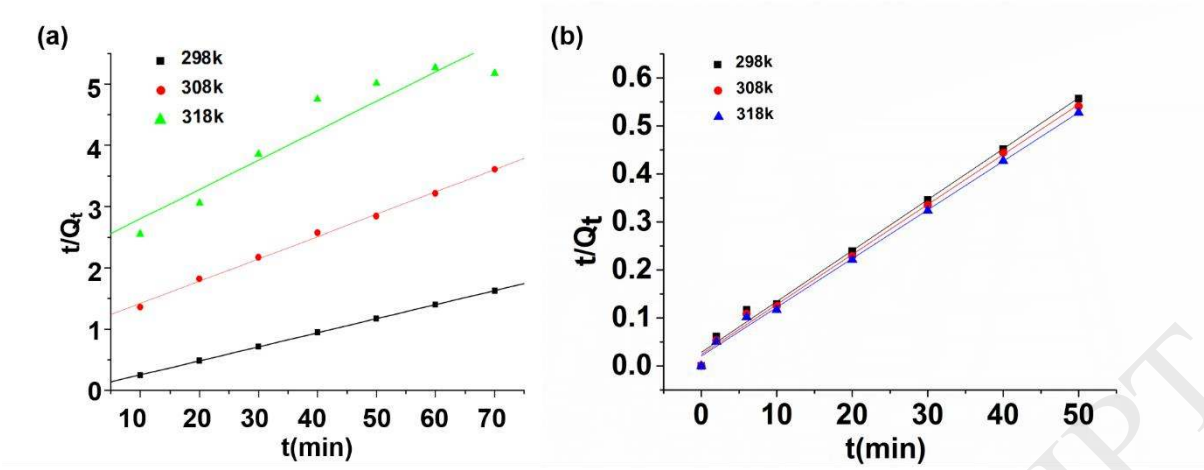

Fig. 10 Plots of pseudo-second-order kinetics for the adsorption of MG(a) and Pb^{2+}(b).

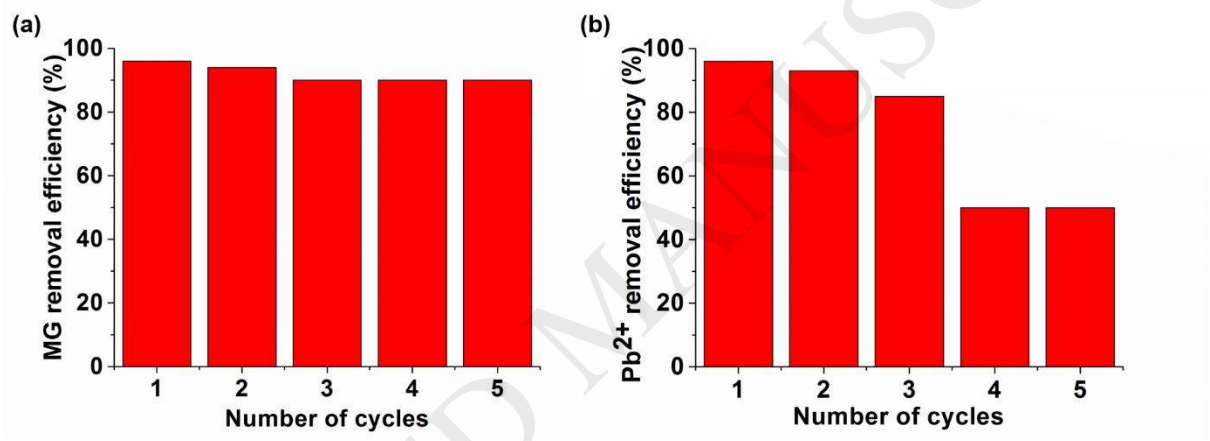

Fig. 11 Recyclability of Cu-MOFs/Fe_3O_4 composite for MG and Pb^{2+} adsorption.

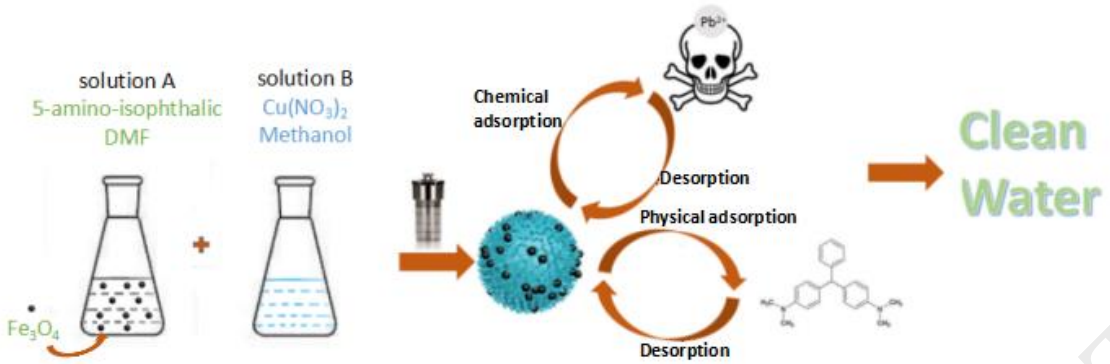

Scheme 1 Schematic illustration the synthesis of Cu-MOFs/Fe_3O_4 composite for removal of MG and Pb(II).

Table1 Comparison of the Maximum adsorption capacity

Sample	Adsorbents	Adsorption capacity (mg/g)	References
Pb^{2+}	γ-Fe_2O_3 nanoparticles	48.90	[38]
	Fe_3O_4@SiO_2-EDTA	114.94	[39]
	Fe_3O_4/Cu-MOFs	219.00	This work
MG	Avena sativa (oat) hull	83.00	[40]
	Diatomite	23.64	[41]
	Fe_3O_4/Cu-MOFs	113.67	This work

Table 2 Relative parameters of thermodynamic equilibrium.

Sample	T(K)	K	$\Delta H(kJ\cdot mol^{-1})$	$\Delta S(J\cdot mol^{-1}\cdot K^{-1})$	$\Delta G(kJ\cdot mol^{-1})$
MG	298	3.26	49.75	176.82	-2.99
	308	6.75			-4.76
	318	11.49			-6.53
Pb^{2+}	298	0.88	28.76	101.39	-1.45
	308	1.19			-2.47
	318	1.83			-3.48

Table 3 Removal efficiency of Cu-MOFs/Fe_3O_4 composite for adsorption MG and Pb^{2+} in real water sample. Final concentration of the solution before (a) and after (b) adsorption by Cu-MOFs/Fe_3O_4 composite.

Sample	Added	Concentration (mg L^{-1})[a]	Found (mg L^{-1})[b]	Removal efficiency (%)
1	Pb^{2+}	100.00	13.25	86.75
	MG	46.35	3.83	91.73
2	Pb^{2+}	10.00	0.70	93.00
	MG	46.35	3.24	93.01
3	Pb^{2+}	100.00	12.46	87.54
	MG	4.64	0.47	89.92
4	Pb^{2+}	10.00	0.57	94.35
	MG	4.64	0.39	91.49